

VARYING POROSITY KINETIC MODEL FOR DIRECT AND REACTIVE SOLID-LIQUID EXTRACTION

I. SEIKOVA and A. MINTCHEV

(Department of Chemical Engineering, University of Chemical Technology and Metallurgy, blvd. Kilment Ohridski 8,
1756 Sofia, BULGARIA)

Received: April 23, 2001

A mathematical model is presented accounting for the effects of porosity increase during extraction from vegetable materials. The relation between the porosity and the total extract release is derived from the solid phase volume balance. The model will be used to interpret the experimental data for alkaloid recovery from leaves and radix of the medicinal plant *Atropa Belladonna*. The extractability has been determined by dissolution of alkaloidic salts in polar solvent (direct extraction) and by alkaline transformation of salts to bases in non-polar solvent (reactive extraction). Supporting experiments were performed in order to estimate the kinetics of solvent penetration. For inert conditions, the estimated effective diffusivities are nearly equal to those obtained under reaction conditions. The resorted differences in the diffusivity as a result of the porosity changes remain lower in respect to the strong influence of the different initial pore structure of the two raw materials.

Keywords: solid-liquid extraction, vegetable alkaloid recovery, chemical reaction, porous medium, liquid penetration

Introduction

Solid-liquid extraction coupled by chemical or biochemical reaction occurs frequently during valorisation of natural materials [1-2]. Generally the kinetics of the process is represented by macroscopic mass balance on the overall solid phase with volume reaction models:

$$\frac{\partial C_2}{\partial t} = D_{eff} \nabla^2 C_2 + R_v \quad (1)$$

where R_v is the rate of chemical reaction per unit volume and $C_2(t,r)$ represents the concentration of the diffusing reaction product. This equation allows a constant effective diffusivity D_{eff} to be estimated assuming that the initial structure of the porous solid is maintained while the extraction proceeds.

In many cases during the treatment of the vegetable material several additional processes, as co-solutes migration, solvent adsorption, hydration or other reactions occur simultaneously with valuable component mass transfer. The structure of the solid can be readily affected and this is accompanied generally by a porosity increase. Varying porosity causes an increase in the diffusivity with the course of the extraction. Theoretical studies have revealed that the ratio of effective diffusivity to molecular diffusivity varies

proportionally by $\varepsilon_p^{1.3-3}$ depending on the adopted geometric description of the pore structure [3-6].

Initial experiments with the considered plant indicated sizeable amounts of dissolved co-solutes. In parallel an increase of the volume of solvent penetrating in the solid was resorted that differed for the various solvents that were used [7]. Then, the measurement and evaluation of the porosity effect are important for the accurate prediction of the values of D_{eff} under reactive or inert conditions.

In the present paper a dynamic model is proposed to describe the diffusive-reactive phenomena when the porosity increases with the course of the extraction. To predict the porosity changes a simplified model is adopted that relates the kinetics of solvent penetration to the kinetics of release of the total extract. The presented model will be used to interpret the experimental data of kinetics of alkaloid recovery by direct and reactive extraction from different parts of the medicinal plant *Atropa belladonna* in a batch system.

Mathematical model

The overall process of extraction with simultaneous chemical reaction involves consideration of the following phenomena:

- (a) chemical conversion of insoluble compound that is initially adsorbed or chemically bounded in a solid to soluble reaction product, prior to its diffusion through the pore space;
- (b) parallel release of all-soluble compounds initially present accompanied by additional solvent penetration and porosity increase.

The approximate model is derived under the following assumptions:

- the solid represents one monodispersed phase of spherical particles with mean radius R_s and initial porosity $\varepsilon_{p,0}$; the particles retain their shape and dimension during reaction and extraction, although the porosity increases;
- the extractable compounds are uniformly distributed in the porous solid particles;
- the solid-solvent phases ratio β is high, so that the solutions are always dilute and density variations and multicomponent effects on the diffusion are negligible;
- the analysis is restricted to first-order irreversible reaction that takes place all over the solid volume without participation of the pores, according to the rate equation:

$$\frac{dC_s(t)}{dt} = -k_r C_s (1 - \varepsilon_p) \quad (2)$$

where $k_r = f(pH, T)$ is the effective reaction rate constant.

Under varying porosity condition the transient diffusion of the soluble reaction product within the particle obeys the following relationship [8]:

$$\frac{\partial(\varepsilon_p C_p)}{\partial t} = \frac{1}{r^2} \frac{\partial}{\partial r} \left(D_{eff}(\varepsilon_p) r^2 \left(\frac{\partial C_p}{\partial r} \right) - C_p v_r \right) + k_r C_s (1 - \varepsilon_p) \quad (3)$$

The solvent radial velocity v_r in the pores can be related to the porosity increase from the continuity equation:

$$\frac{\partial \varepsilon_p}{\partial t} + \frac{1}{r^2} \frac{\partial}{\partial r} (r^2 v_r) = 0 \quad (4)$$

After integration of the continuity equation and substituting this in Eq.(3) the conservation equation takes the form:

$$\frac{\partial(\varepsilon_p C_p)}{\partial t} = \frac{1}{r^2} \frac{\partial}{\partial r} \left(D_{eff}(\varepsilon_p) r^2 \frac{\partial C_p}{\partial r} \right) - \left(\frac{d\varepsilon_p}{dt} \right) \frac{1}{r^2} \frac{\partial}{\partial r} (r^3 C_p) + k_r C_s (1 - \varepsilon_p) \quad (5)$$

The associated boundary conditions are:

$$\left(\frac{\partial C_p}{\partial r} \right)_{r=0} = 0 \quad (6)$$

$$-D_{eff} \left(\frac{\partial C_p}{\partial r} \right)_{r=R_s} + (v_r C_p)_{r=R_s} = k_m (C_p|_{r=R_s} - C_1(t)) \quad (7)$$

In the last step of the process, the solute is transported from the pores opening on the contact surface to the bulk liquid phase at concentration $C_1(t)$:

$$\frac{dC_1(t)}{dt} = \frac{3}{R_s} k_m \beta (C_p|_{r=R_s} - C_1(t)) \quad (8)$$

Solid phase volume balance may be used as theoretical possibility to correlate the changes in a pore volume with the amount of compounds released [9]. It is known that solvent penetration in the pore space is the initial stage of the extraction. It is assumed that an initial porous volume $\varepsilon_{p,0} V_s$ is immediately filled with solvent. With the disappearance of extractable compounds from the solid the free space volume inside the particles increases and the solvent penetration continues during the whole stage of the extraction.

The solid phase apparent volume V_s consists of inert solid matter V_{in} , pore volume filled with solvent $V_{ls}(t)$ and extractable compounds $V_{ext}(t)$:

$$V_s = V_{in} + V_{ls}(t) + V_{ext}(t) \quad (9)$$

The solvent volume impregnated the solid is represented by the varying porosity:

$$V_{ls}(t) = \varepsilon_p(t) V_s \quad (10)$$

The decrease in the volume of the extractable compounds $V_{ext}(t)$ may be expressed through the amount extracted for the time t . Generally, the extract increases in time $m_{ext} = f(t)$, it can be described by sufficient accuracy by equation of the type:

$$m_{ext}(t) = A - B \exp^{-Ht} \quad (11)$$

where A , B and H are empirical coefficients. Then the unextracted fraction in the solid phase $\gamma(t)$ is defined from the total balance:

$$\gamma(t) = 1 - \frac{m_{ext}(t)}{X_0 m_0} \quad (12)$$

where the initial mass fraction X_0 is established experimentally after multiple treatment with fresh solvent. The particular volumes can be expressed as follow:

$$V_{ext}(t) = \frac{X_0 m_0 - m_{ext}(t)}{\bar{\rho}_{ext}} = \frac{\gamma(t) X_0 m_0}{\bar{\rho}_{ext}} \quad (13)$$

$$V_{in} = \frac{m_{in}}{\bar{\rho}_{in}} = \frac{(1 - X_0) m_0}{\bar{\rho}_{in}} \quad (14)$$

Introducing Eqs.(10), (13) and (14) into Eq.(9) gives:

$$V_s = \frac{m_0}{1 - \varepsilon_p} \left(\frac{1 - X_0}{\bar{\rho}_{in}} + \frac{\gamma X_0}{\bar{\rho}_{ext}} \right) \quad (15)$$

When the changes in the dimension of the solid particles are negligible, solvent penetration equals the volume of the disappearance of extractable compounds. The porosity changes in a function of time is given by the following relationships:

$$\varepsilon_p(t) = 1 - (1 - \varepsilon_{p,0}) \frac{\frac{1 - X_0 + \gamma(t)X_0}{\bar{\rho}_{in}} - \frac{\bar{\rho}_{ext}}{1 - X_0 + X_0}}{\frac{\bar{\rho}_{in}}{\bar{\rho}_{ext}}} \quad (16)$$

The porosity changes would affect the solute diffusivity. An exponential increase in the effective diffusivity in respect to the extracted fraction $(1-\gamma)$ is assumed and it is defined by the following empirical function:

$$D_{eff} = D_{eff,0} \exp^{\alpha(1-\gamma)} \quad (17)$$

where α is a numerical constant and $D_{eff,0}$ is the effective diffusivity evaluated for the initial conditions.

The system of Eqs. (2-17) can be rearranged to a dimensionless form:

$$\frac{dC_1^*(\tau)}{d\tau} = -Th^2 C_1^* \quad (18)$$

$$\frac{\partial(\varepsilon_p C_1^*(\tau, \varphi))}{\partial \tau} = D^* \frac{1}{\varphi^2} \frac{\partial}{\partial \varphi} \left(\varphi^2 \frac{\partial C_1^*}{\partial \varphi} \right) - \left(\frac{d\varepsilon_p}{d\tau} \right) \frac{1}{\varphi^2} \frac{\partial}{\partial \varphi} \left(\frac{\varphi^3}{3} C_1^* \right) + Th^2 C_1^* \quad (19)$$

$$\frac{dC_1^*(\tau)}{d\tau} = 3Bi\beta \left(C_1^*|_{\varphi=1} - C_1^* \right) \quad (20)$$

$$\text{I.C. } C_1^*(0) = 1, \quad C_1^*(0, \varphi) = 0, \quad C_1^*(\infty) = 0 \quad (21)$$

$$\text{B.C. } \left. \frac{\partial C_1^*}{\partial \varphi} \right|_{\varphi=0} = 0 \quad (22)$$

$$-D^* \left. \frac{\partial C_1^*}{\partial \varphi} \right|_{\varphi=1} + \frac{\varphi}{3} \frac{d\varepsilon_p}{d\tau} = Bi \left(C_1^*|_{\varphi=1} - C_1^* \right) \quad (23)$$

with the following dimensionless parameters:

$$\varphi = \frac{r}{R_s}, \quad C^* = \frac{C}{C_{s,0}}, \quad \beta = \frac{V_s}{V_l},$$

$$D^* = \frac{D_{eff}}{D_{eff,0}} = \exp^{\alpha(1-\gamma)}, \quad \tau = \frac{D_{eff,0}}{R_s^2} t, \quad (24)$$

$$Bi = \frac{k_m R_s}{D_{eff,0}}, \quad Th = R_s \sqrt{\frac{(1-\varepsilon_p)k_r}{D_{eff}}},$$

where Th is called Thiele-type modulus for the porous particle that brings out the relative significance of the reaction rate [10,11].

Numerical treatment

The coupled system of second order, partial and ordinary differential equations of the presented model is solved numerically. Four-order Runge-Kutta method was utilized for the ordinary differential equations. The

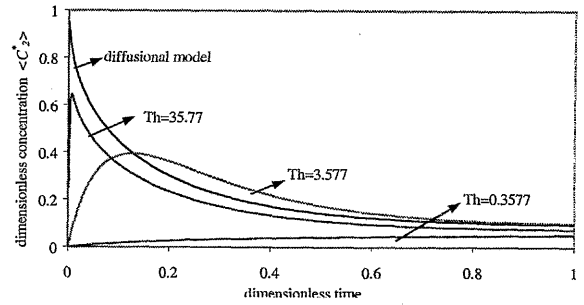


Fig.1 Reaction rate constant influence on the averaged concentration in the solid phase (computed for $Bi=400$, $k_r = 0.8 \text{ s}^{-1}$, $0.8 \cdot 10^{-2} \text{ s}^{-1}$ and $0.8 \cdot 10^{-4} \text{ s}^{-1}$)

approach for the parabolic partial differential equations is based on Crank-Nikolson finite difference scheme. For the resolution of the resulting systems of algebraic equations forward-backward Thomas' algorithm was used.

From the dimensionless mass balance of the solid particle Eq.(19) it is clear that Thiele modulus, the magnitude of variation in porosity ε_p and effective diffusivity D^* will control the process. The integration of this equation around the overall solid particle volume yields the evolution of the averaged concentration $\langle C_2^* \rangle$ in the particle:

$$\frac{d}{dt} \langle C_2^* \rangle = \frac{\partial}{\partial \tau} \left(\int_V \varepsilon_p C_1^* \right) = \left(D^* \frac{\partial C_1^*}{\partial \varphi} \right)_{\varphi=1} - \left(\frac{\partial \varepsilon_p}{\partial \tau} \right) \frac{1}{\varphi^2} \frac{\partial}{\partial \varphi} \left(\frac{\varphi^3}{3} C_1^* \right) + Th^2 C_1^* \quad (25)$$

The values of this term can be positive or negative depending on the relative magnitude of the rate of diffusion and chemical reaction. Fig.1 shows the plots $\langle C_2^* \rangle = f(t)$ computed for specific ranges of Thiele modulus. The curves are compared with the prediction provided from a pure diffusional model. In the usual situation for large Biot numbers there can be distinguished three different kinetic regimes:

- diffusion-controlling regime ($Th \gg 1$): in case of instantaneous or very fast chemical reaction the conversion takes place before the solute can diffuse into the interior of the particle; the effect of reaction rate is negligible and the disappearance of the solute is a continuously decreasing function;
- reaction-diffusion regime ($Th > 1$): the diffusion of solute is not fast enough to compensate for its appearance by reaction and the evolution of the concentration $\langle C_2^* \rangle$ passes through a maximum before the reactant is completely converted;
- reaction rate-controlling regime ($Th < 1$): the slow consumption of the reactant in respect to the product diffusion leads to slowly increasing accumulation inside the particle volume.

The effect of the interaction reaction-diffusion on the kinetic curves $C_1^* = f(\tau)$ in the liquid phase is shown in Fig.2. As a result of the resistance induced by the chemical reaction the kinetic curves that are normally convex under diffusion-controlling regime take a sigmoidal form, when the rate of reaction is comparable with the diffusion rate. For large values of Thiele

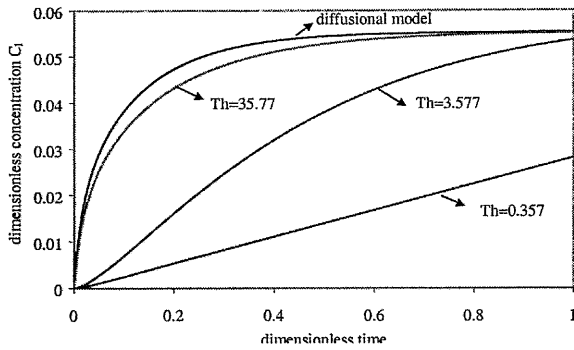


Fig. 2 Reaction rate constant influence on the concentration in the liquid phase (computed for $Bi=400$, $k_r=0.8\text{ s}^{-1}$, $0.8\cdot 10^{-2}\text{ s}^{-1}$ and $0.8\cdot 10^{-4}\text{ s}^{-1}$)

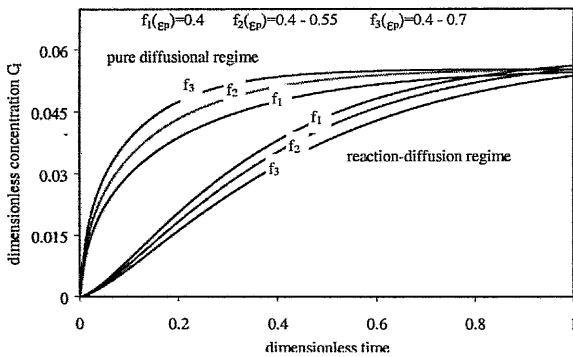


Fig. 3 The effect of the varying porosity under non-reactive and reactive conditions ($Th=3.577$, $k_r=0.8\cdot 10^{-2}\text{ s}^{-1}$)

modulus ($Th>40$) the prediction approaches an asymptotic curve controlled purely by pore diffusion. Physically, for given particle size and reaction rate constant, the parameter Th increases as the effective diffusivity D_{eff} is decreased:

- using porous solid of very small pore size;
- using porous solid having a small porosity or high tortuosity factor.

The effect of the varying porosity under reaction or non-reaction conditions is explained by these considerations. In Fig. 3 are presented the computed values of dimensionless concentration in the liquid phase $C_i^*(\tau)$ for both diffusion-controlling and reaction-diffusion regime with porosity as parameter. The kinetic behavior is simulated for three cases: constant porosity ($\varepsilon_p=0.4$), moderate ($\varepsilon_p=0.4+0.55$) and very marked porosity change ($\varepsilon_p=0.4+0.7$).

As expected, under diffusion-controlling regime the higher the porosity the faster the overall extraction process. However, under reaction-diffusion regime a delay in the process is predicted as the porosity is increased. The increasing values of the porosity ε_p and the effective diffusivity D_{eff} lead to a decrease in the values of Th . When the rate of reaction is decreased in respect to the diffusion rate, the concentration gradient at the solid-liquid interface declines rapidly and this effect is not completely compensated by the increasing D_{eff} .

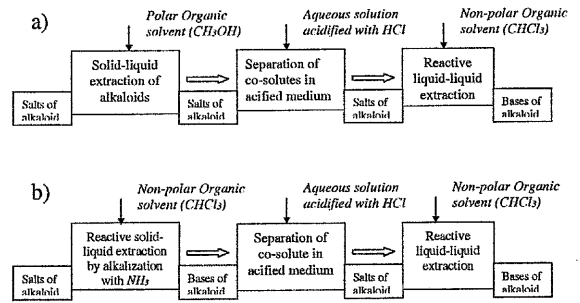


Fig. 4 Steps of alkaloid recovery from *Atropa Belladonna* plant: a) Direct solid-liquid extraction; b) Reactive solid-liquid extraction

As a result from the contradictory effect of the varying porosity erroneous results can be obtained using a model with constant porosity, namely an apparent decrease in D_{eff} when the reaction is carried out in a reaction-diffusion regime.

Experimental

Exemplary vegetable alkaloid recovery by direct or reactive extraction has been studied. Small quantities of tropan alkaloids are found in leaves, seeds and radix of the medicinal plant *Atropa Belladonna*. These are predominantly in alkaloidic salt form and dissolved in the cellular liquid. The known methods for alkaloid extraction are based on their different solubility according to solvent polarity. The polar organic solvents are appropriate solvents for alkaloid salts. When using non-polar solvent, alkaloid bases dissolve. The co-solutes are also selectively removed. Unvaluable substances, as polysaccharides, mineral salts, tanins, flavanoids dissolve in ethanol. Chloroform extracts contain non-polar substances: chlorofils, acids, fatty oils, pigments. The overall process consists of the following stages (Fig. 4):

1. Solid-liquid extraction by direct dissolution of salts in polar solvent (direct extraction) or by prior alkaline transformation of salts to bases in non-polar solvent (reactive extraction).
2. Extract purification from associated co-solutes by acidic treatment with aqueous solution.
3. Crude-alkaloids recovery from the cleaned-up extract by alkaline transformation in alkaloid bases.

In the experimental study the solvent was methanol for direct extraction, and chloroform under reaction conditions. Adjustment of pH alkaline of the solution was made by means of 25% NH_3 . For acidification of the aqueous solutions 8% HCl was used. Alkaloids were extracted from dried and fractionated samples, provided from two different parts of the plant, namely radix and leaves. The structure of the porous solid was investigated by nitrogen adsorption at 77.4 K by the simplified single-point BET procedure. The results show that the pore spaces of the epigeous and subterraneous tissues strongly differ in their structural parameters:

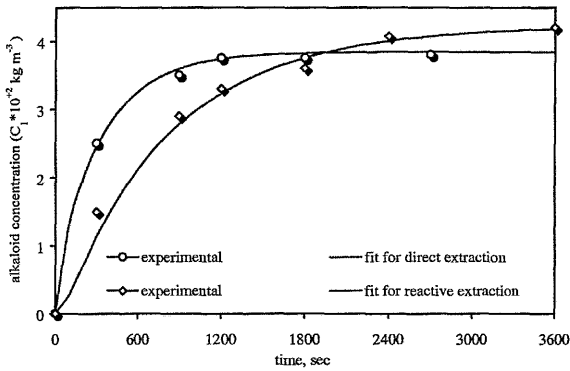


Fig.5 Course of extraction $C_I=f(t)$ from radix samples

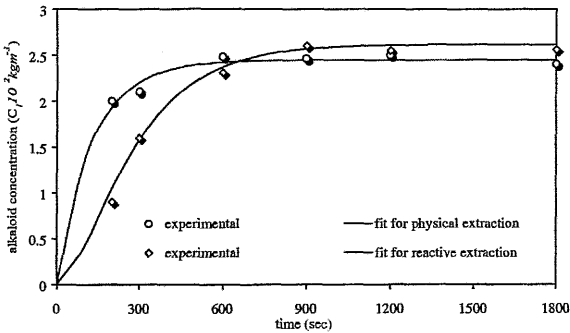


Fig.6 Course of extraction $C_I=f(t)$ from leaves samples

- leaves: specific area $1.7 \text{ m}^2 \text{ g}^{-1}$, free volume $0.6 \text{ m}^3 \text{ g}^{-1}$, mean pore radius 11 nm.
- radix: specific area $0.4 \text{ m}^2 \text{ g}^{-1}$, free volume $0.15 \text{ m}^3 \text{ g}^{-1}$, mean pore radius 16 nm.

The initial content of alkaloids was obtained after continuous extraction in a Soxhlet apparatus: 0.3% of the dried mass for leaves and 0.6% for radix. The experimental procedure has been divided in two groups. The first one analyses the recovery of the alkaloids in the cleaned-up extracts to provide the kinetic curves $C_I=f(t)$. For this aim the solutions were analysed for alkaloids by spectrophotometric measurement at wavelength $\lambda=430 \text{ nm}$ [12-13].

The second group investigates the kinetics of total extract removal and solvent penetration. The observations include simply measuring the changes in weight: when the pores are filled with a solvent (m_{s1}), and after removing the impregnated solvent by drying at $40 \text{ }^\circ\text{C}$ for about 12 hours (m_{s2}). From this experimental values the kinetics of total extract release $m_{ext}=f(t)$ and the volume of solvent penetrating into the porous material $V_{is}=f(t)$ can be determined by noting that:

$$m_{ext}(t) = m_{s0} - m_{s2}(t) \quad (26)$$

$$V_{is}(t) = \frac{m_{s1}(t) - m_{s2}(t)}{\rho_1} \quad (27)$$

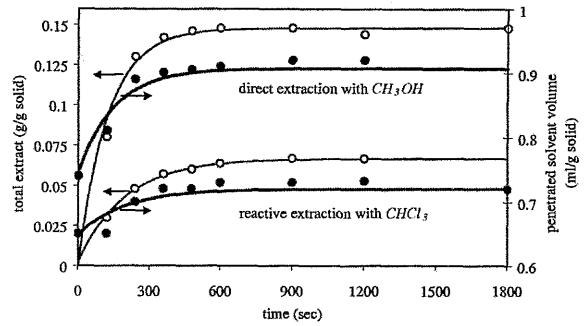


Fig.7 Experimental and predicted total extract and solvent penetration increase during direct and reactive extraction of radix samples

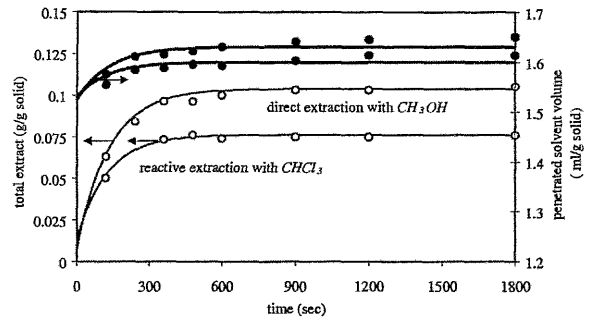


Fig.8 Experimental and predicted total extract and solvent penetration increase during direct and reactive extraction of leaves samples

Results and Discussions

Kinetic experiments were carried out in a stirred batch reactor, at $25 \text{ }^\circ\text{C}$, under the following conditions: hydromodulus $\eta=0.09 \text{ m}^3 \text{ kg}^{-1}$, particles mean size $R_s=0.5 \cdot 10^{-3} \text{ m}$, extraction time $t_{max}=3600 \text{ s}$ for radix samples and $t_{max}=1800 \text{ s}$ for leaves. Rotation speed of 4 revolutions s^{-1} assures internal diffusion-controlling process under inert conditions. Figs.5 and 6 show the course of direct and reactive extraction of alkaloid $C_I=f(t)$ obtained respectively from radix and from leaves. The symbols are the experimental points, the curves represent the best-fit simulation results.

It is evident that the extraction from leaves samples is achieved more easily: the time of equilibration is 2 time smaller and the drawing out alkaloids is more complete: 87% degree of recovery with 72% from the radix. The effect of chemical reaction depicts an identical trend for the two raw materials: shift to sigmoidal extraction-time behaviour characterized by decline of the extraction rate in the early stage of the process, followed by steep increase. The total amount of crude alkaloids gained with chemical reaction is slightly increased. The facts prove that some alkaloids are not originally in salt form, and these bounded in other forms are extracted by chemical reaction.

For the different methods of extraction the amounts of the total extract may be varying because of the different dissolving activities. The experimental data for the total extract per unit mass of solid $m_{ext}^*=f(t)$ thus

Table 1 Fitted values for model parameters in case of constant or varying porosity

| | Plant radix samples | | | | Plant leaves samples | | | |
|-------------------------------|---------------------------|-----------------------|---------------------------|-----------------------|---------------------------|-----------------------|---------------------------|-----------------------|
| | reactive extraction | | direct extraction | | reactive extraction | | direct extraction | |
| | $\varepsilon_p=f(\gamma)$ | $\varepsilon_p=const$ | $\varepsilon_p=f(\gamma)$ | $\varepsilon_p=const$ | $\varepsilon_p=f(\gamma)$ | $\varepsilon_p=const$ | $\varepsilon_p=f(\gamma)$ | $\varepsilon_p=const$ |
| $k_r, 10^2 s^{-1}$ | 1.89 | 1.16 | - | - | 1.46 | 1.76 | - | - |
| $D_{eff}, 10^{10} m^2 s^{-1}$ | 1.32 | 0.78 | 1.45 | 2.89 | 8.46 | 7.15 | 8.62 | 9.22 |
| $\alpha (Eq.17)$ | 2.6 | - | 2.3 | - | 0.9 | - | 1.1 | - |
| Th | 4.6-3.6 | 4.72 | - | - | 1.3-1.2 | 1.43 | - | - |

obtained is shown by the points in Figs.7 and 8. The following empirical relationships were deduced:

$$m_{ext}^* = 0.148 - 0.139 \exp^{-0.00655t} \quad (28)$$

(from radix with methanol)

$$m_{ext}^* = 0.0669 - 0.0586 \exp^{-0.00725t} \quad (29)$$

(from radix with chloroform)

$$m_{ext}^* = 0.106 - 0.94 \exp^{-0.0083t} \quad (30)$$

(from leaves with methanol)

$$m_{ext}^* = 0.0764 - 0.0631 \exp^{-0.00844t} \quad (31)$$

(from leaves with chloroform)

A steep increase in the amount of total extract is recorded in the early stage of the process. The same figures represent the comparison between measured (by points) and predicted values (continuous lines) of the volume of the solvent impregnated the solid. The experimental observations confirm that the solvent continuously penetrates in the solid during extraction. The higher the initial porosity, the greater the initially penetrated solvent volume, but its relative increase during extraction is lower. For direct extraction from radix, the methanol penetrated in the solid increases from 0.767 to 0.901 ml/g solid that represents porosity increases between 0.4-0.56. With the increasing penetrated volume from 1.52 to 1.64 ml/g solid for leaves, the porosity is increased only from 0.6 to 0.65. Lower porosity variation was recorded during treatment with chloroform: in the range $\varepsilon_p=0.39-0.47$ for radix and $\varepsilon_p=0.6-0.63$ for leaves.

The experimental data for the kinetics of solvent penetration is very near to the predicted from the particle volume balance. Thus, although the experimental data is not sufficiently detailed, it seems that the presented approach is able to determine approximately the range of the porosity increase.

The above experimental procedure forms the basis for the estimation of the kinetic parameters (Table 1). To highlight the possible effects of porosity increase, the values of the adjustable parameters, obtained by the varying porosity model reported here ($\varepsilon_p=f(\gamma)$), are compared with the values obtained in constant porosity model ($\varepsilon_p=\varepsilon_{p,0}$). The following conclusions can be made:

- The values of the reaction rate constant k_r are almost identical and remain independent from the solid phase structure. During extraction from radix, or from leaves, the transition from diffusional to mixed diffusion-reaction regime is registered.
- For the same raw material the values of D_{eff} for reacting system were predicted to be smaller than those for inert system using constant porosity model. In order to predict the same rate of extraction at a lower porosity, in diffusion-controlling regime an increased D_{eff} has to be used in the constant porosity model. In contrast, in a mixed diffusion-reaction regime, an apparently lower D_{eff} will be calculated. When the varying porosity model is used, identified diffusion coefficients using polar or non-polar solvent are similar. This result seems to be more realistic, since the two solvents have approximately the same viscosity and the solute concentrations are in the same order of magnitude.
- In case of direct, or reactive extraction, the diffusivity D_{eff} in the porous particles from leaves are higher than those from radix - the factor between the coefficients is in the range 7-8. The larger D_{eff} suggests lower tortuosity factor and more regular pore structure of the leaves samples.

The identified values of the adjustable numerical constant α in Eq.(17) show much larger increase in D_{eff} in case of lower initial porosity. It is obvious that liquid penetration affects also the interconnectivity of the pores and the tortuosity factor is decreased. Appreciable differences in the effective diffusivity were obtained, considering or not porosity increase, for the kinetic behavior of radix samples where porosity increase is greater than 20%. The major deviation of about 200% in the effective diffusivity was obtained for direct extraction from radix when the total extract remove reached 15%.

For the examined solid-liquid system dimension increase and swelling of the porous particles is not observed and the penetrated solvent volume remains relatively low. The resorted differences in D_{eff} as a result of the porosity increase remain lower in respect to the strong influence of the initial pore structure.

Conclusion

A dynamic model with variable transport properties is presented to predict the kinetic behaviour during direct or reactive extraction from vegetable material. Starting

point is the experimentally recorded kinetics of solvent penetration and total extract release. The variation of the porosity with the total extract release is taken into account. An exponential increase in the effective diffusivity with the evolution of the fraction extracted is considered.

To exploit the model suitability, the extractibility of alkaloids from the medicinal plant *Atropa belladonna* has been reported. Different kinetics of extraction of alkaloids was obtained for the different parts of the plant using different method for valuable compound liberation. Using chemical reaction the equilibration delays about 2 times in respect to the direct dissolution, without sensible increase in the recovery degree. Using ethanol, or chloroform as solvent under direct or reactive reaction the estimated values for the effective diffusivities are independent of the method of dissolution, but they depend very strongly on the initial structure of the pore space. The values of effective diffusion calculated at 25 °C varies in the range $1.32 \cdot 10^{-10} \text{ m}^2 \text{ s}^{-1}$ for radix to $8.62 \cdot 10^{-10} \text{ m}^2 \text{ s}^{-1}$ for leaves.

The resorted differences in the kinetic behaviour show that it may be advantageous to characterize porous media changes directly by measuring the kinetics of solvent penetration. While the commonly used techniques of pore space determination, as mercury porosimetry or B.E.T. gas adsorption allows investigation only of dry material, the experimental kinetics of liquid impregnation provides direct information about swelling properties of the solvent and eventual structural changes with advancement of the extraction. The presented approach can be extended to include the particle dimension changes when considerable swelling is observed and the resorted effects are more obvious.

SYMBOLS

| | |
|-----------------------|--|
| a_s | specific external area, $\text{m}^2 \text{ m}^{-3}$ |
| Bi | Biot number ($=k_m R_s / D_{eff,0}$) |
| C_1 | solute concentration in bulk liquid phase, kg m^{-3} |
| C_p | solute concentration in pores of particle, kg m^{-3} |
| $\langle C_2 \rangle$ | volume-averaged concentration in solid phase, kg m^{-3} |
| C_s | transformable compound concentration in solid phase, kg m^{-3} |
| C^* | dimensionless concentrations |
| D_{eff} | effective diffusivity, $\text{m}^2 \text{ s}^{-1}$ |
| $D_{eff,0}$ | effective diffusivity at initial porosity, $\text{m}^2 \text{ s}^{-1}$ |
| D^* | factor for effective diffusivity increase ($=D_{eff} / D_{eff,0}$) |
| k_r | chemical reaction rate constant, s^{-1} |
| k_m | external mass transfer coefficient, m s^{-1} |
| m_0 | initial mass of solid phase, kg |
| m_{in} | mass of inert compounds in the solid phase, kg |
| m_{ext} | mass of extracted compounds, kg |
| m^*_{ext} | mass of extracted compounds per unit of dried solid, kg kg^{-1} |

| | |
|-----------|---|
| m_{sl} | common mass of solid phase, impregnated with solvent, kg |
| m_{ss} | mass of solid phase after removing solvent excess, kg |
| r | radial coordinate, m |
| R_v | volume reaction rate, $\text{kg m}^{-3} \text{ s}^{-1}$ |
| R_s | particle radius, m |
| Th | Thiele-type modulus ($=R_s \sqrt{(1-\varepsilon_p)k_r/D_{eff}}$) |
| X_o | initial mass fraction of extractable compounds, kg kg^{-1} |
| V_{ext} | extractable compounds volume, m^3 |
| V_{in} | inert compounds volume, m^3 |
| V_l | liquid phase volume, m^3 |
| V_{ls} | solvent volume in the solid phase pores, m^3 |
| V_s | solid phase apparent volume, m^3 |
| v_r | solvent radial velocity in the pores, m s^{-1} |

Greek Letters

| | |
|---------------------|---|
| α | empirical constant defined by Eq.(17) |
| β | phase ratio ($=V_s/V_l$) |
| γ | fraction of unextracted compounds |
| ε_p | porosity of the particle |
| $\varepsilon_{p,0}$ | initial porosity of the particle |
| φ | relative coordinate |
| λ | wavelength, nm |
| η | hydromodulus ($=V_l/m_o$), $\text{m}^3 \text{ kg}^{-1}$ |
| τ | dimensionless time ($=D_{eff,0}t/R_s^2$) |

REFERENCES

1. MINKOV S., MINTCHEV A. and PAEV K.: J. of Food Engineering, 1996, 29, 107-113
2. GOTO M., SMITH J. M. and MCCOY B. J.: Chem. Eng. Sci., 1990, 45 (2), 443-448
3. RAMACHANDRAN P. A. and SMITH J. M.: Chem. Eng. J., 1977, 14, 137-146
4. FAN L. S., MIYANAMI K. and FAN L. T.: Chem. Eng. J., 1977, 11, 13-20
5. HPOLLEWAND M. P. and GLADDEN L. F.: Chem. Eng. Sci., 1992, 47 (7), 1761-1770
6. MARMUR A. and COHEN R.: J. of Colloid and Interface science, 1997, 189, 299-304
7. SEIKOVA I., GUIRAUD P. and MINTCHEV A.: Comptes rendues de l'Academie Bulgare des Sciences, 2000, 53(3), 55-58
8. TRIDAY J. and SMITH J. M.: AICh J., 1988, 34 (4), 658-668
9. HINZ Th. and EGGERS R.: Nahrung , 1996, 40 (3), 116-124
10. SATTERFIELD C. N.: Heterogeneous Catalysis in Practice, McGraw-Hall, New York, p.87-119, 1980
11. MCGREAVY C., ANDRADE J. S. and RAJAGOPAL K.: Chem. Eng. Sci. 1992, 47 (9-11), 2751-2756
12. SOKOLOV A. V. and POPOV D. M.: Farmatsiya (Moscow), 1989, 38 (6), 62-65
13. GRISHINA M. S., DYUKOVA V. V., KOVALENKO L. I. and POPOV D. M.: Khim.-Farmatsiya Zh. (Moscow), 1985, 19 (9) ,1102-1105